ZnO-based film bulk acoustic resonator for high sensitivity biosensor applications

Z. Yan
Laboratory of Nano-Technology, Shanghai Institute of Microsystem and Information Technology, Chinese Academy of Science, Shanghai 200050, China; Department of Applied Physics, The Hong Kong Polytechnic University, Hong Kong, China; and Materials Research Center, The Hong Kong Polytechnic University, Hong Kong, China

X. Y. Zhou and G. K. H. Pang
Department of Applied Physics, The Hong Kong Polytechnic University, Hong Kong, China and Materials Research Center, The Hong Kong Polytechnic University, Hong Kong, China

T. Zhang, W. L. Liu, J. G. Cheng, Z. T. Song, and S. L. Feng
Laboratory of Nano-Technology, Shanghai Institute of Microsystem and Information Technology, Chinese Academy of Science, Shanghai 200050, China

L. H. Lai and J. Z. Chen
School of Life Science, East China Normal University, Shanghai 200062, China

Y. Wang[a)]
Department of Applied Physics, The Hong Kong Polytechnic University, Hong Kong, China and Materials Research Center, The Hong Kong Polytechnic University, Hong Kong, China

(Received 5 January 2007; accepted 26 February 2007; published online 2 April 2007)

Zinc oxide (ZnO)-based film bulk acoustic resonator consisting of a piezoelectric element (Au/ZnO/Pt) and a Bragg reflector (ZnO/Pt multilayer structure) has been fabricated by magnetron sputtering. The transmission electron microscopy and x-ray diffraction measurements revealed that all thin film layers in the device were well crystallized and highly textured. By electrical measurements, it was found that the device had a high resonant frequency (3.94 GHz) and mass sensitivity (8970 Hz cm^2/ng). The use of the device as a biosensor was demonstrated by comparing the resonant properties of the device with/without coatings of biospecies. © *2007 American Institute of Physics*. [DOI: 10.1063/1.2719149]

Devices with a basic structure of film bulk acoustic resonator (FBAR) have been used as filters in microwave circuits. In recent years, there is an increasing interest to develop FBAR biosensors using a similar technology.[1,2] Consisting of a piezoelectric resonant unit and a Bragg reflector, FBAR has a featured resonance frequency (f_r) which is determined by the structure and size of the device. Application of an external force on the piezoelectric layer induces a shift of f_r and the magnitude of the shift is a function of the external force. Based on this principle, FBAR devices can be used to detect mass changes of biospecies in a biological process/reaction. Compared with quartz crystal microbalances (QCMs), currently the most widely used biosensors, the FBAR biosensors work at a much higher frequency and thus possess a better theoretical sensitivity.[3–5] According to recent journal papers and patents, ZnO-based FBAR biosensors can work at a frequency of up to 2 GHz with a sensitivity of ~2400 Hz cm^2/ng, which is thousand of times better than that of QCMs.[6–12] There is also an effort to develop an alternative piezoelectric material (for example, aluminum nitride) to replace ZnO in the FBAR devices.[13–15] Despite the theory for FBAR structure has been well established and some high sensitivity devices have been reported, there is still large room for further improvement.

Among many factors that may have influence on the comprehensive performance of FBAR device, the property of the ZnO layer in the piezoelectric resonant unit plays a most critical role. It is known that the work frequency (i.e., the resonant frequency) of a typical ZnO-based FBAR can be well estimated using the equation

$$f_r = \frac{1}{2t}\sqrt{\left(\frac{c_{33}^E}{\rho}\right)}\left(\frac{1-0.41k_t^2}{1-0.5k_t^2}\right), \quad (1)$$

where ρ, t, c_{33}^E, and k_t are the density, thickness, stiffness coefficient, and piezoelectric coupling coefficient of the ZnO thin film in the piezoelectric resonant unit, respectively.[16–19] For a ZnO film with a fixed thickness, the three parameters (ρ, c_{33}^E, and k_t) may have different influences on f_r: (1) The typical value of k_t^2 ranges from 7.5% to 8.5%. This variation does not lead to much change in the value of f_r. (2) The density ρ is not a parameter that can be significantly modified, either. (3) Stiffness is the resistance of an elastic body to deflection or deformation by an applied force. Because the ZnO single crystal is highly anisotropic, the actual value of c_{33}^E of a ZnO thin film is dependent on the crystallographic orientation, roughness, and uniformity of thickness of the film. A highly oriented ZnO film with a very smooth surface and good uniformity is beneficial for obtaining a high-f_r device. Quite obviously these requirements are also applicable for all other layers in the Bragg reflector.

In this letter we report our effort on the development of ZnO-based FBAR structure with a higher work frequency

a)Author to whom correspondence should be addressed; electronic mail: apywang@inet.polyu.edu.hk

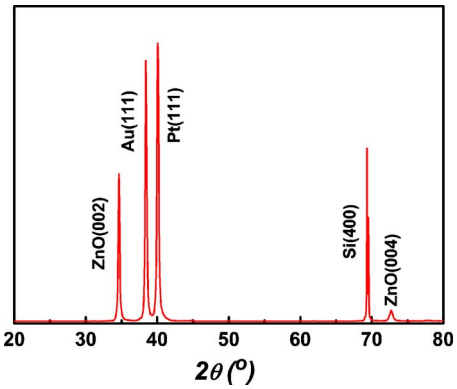

FIG. 1. (Color online) X-ray diffraction pattern of the sample with a layered structure of Au/ZnO/Pt/ZnO/Pt/ZnO/Pt/Si.

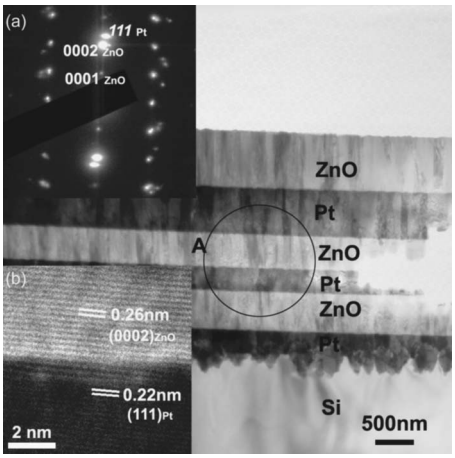

FIG. 2. Cross-sectional observation of ZnO-FBAR in a TEM. The inset (a) shows the selected area electron diffraction pattern and (b) shows a high-resolution image.

and thus a better theoretical sensitivity than reported ones. Our FBAR device consists of a piezoelectric element (Au/ZnO/Pt with thicknesses $t_{Au}=300$ nm, $t_{ZnO}=750$ nm, and $t_{Pt}=500$ nm) and a Bragg reflector (ZnO/Pt/ZnO/Pt/Si with thicknesses $t_{ZnO}=400$ nm, $t_{Pt}=250$ nm, and $t_{Si}=500$ μm). All thin films (Pt, ZnO, and Au) were fabricated via magnetron sputtering using 3 in. targets. The processing conditions were optimized such that ZnO and Pt films with best crystallinity, texture, smoothness, and uniformity could be obtained. The typical deposition parameters include: base vacuum$=2.5\times10^{-4}$ Pa, substrate temperature$=280$ °C, and sputtering power$=200$ W (rf) for ZnO and 100 W (dc) for Pt and Au. The control of thickness of each layer was realized by adjusting the deposition time strictly under the fixed synthesis conditions. The gold top electrodes were patterned using standard microelectronic techniques. Structures of the devices were characterized by x-ray diffraction (XRD) (Bruker AXS D8 Discover), atomic force microscope (Digital Instrument Nanoscope IV), and transmission electron microscopy (TEM) (JEOL JEM-2011) operated at 200 kV.

The electrical characteristics of the devices were studied by measuring the S parameters using a network analyzer (8720ES, Agilent) with a Cascade probe station. Both bare and coated devices were used in the tests. The biospecies for the coating included Staphylococal Protein A mixed with the antibody (goat-antihuman IgG), the sufficient blocking antibody (goat IgG), the antigen (human IgG) for immunoreaction (such as key and lock), and colloidal gold coated with goat-antihuman IgG aiming to augment the total immunoassay mass. During each step, the resonator was thoroughly rinsed with de-ionized water to eliminate uncoated or unreacted mass.

Figure 1 shows the XRD $\theta/2\theta$ scan of our sample (the layered structure is shown later in Fig. 3). Five high intensity peaks were found, which are identified to be ZnO (002), Au (111), Pt (111), Si (004), and ZnO (004) reflections. No other peaks were observed in the test range. Based on the XRD data, it is concluded that all ZnO and Pt layers have good crystallinity and are highly textured. The surface morphology of the sample was checked in an atomic force microscope (data not shown). It was found that the top ZnO layer has a very clean and smooth surface. The average grain size of the ZnO film was ~50 nm and the root-mean-square roughness was ~7 nm.

The cross-sectional structures of the sample were observed in a TEM, which further confirmed the structure features revealed by XRD. Figure 2 shows the bright-field image of the sample with labels on the alternative layers. In the inset of Fig. 2(a), the selected area electron diffraction pattern, taken from the indicated area A, shows the textured growth of ZnO and Pt grains. The ZnO (0002) planes are parallel to the Pt (111) as evident from the indexing on the diffraction pattern. The inset of Fig. 2(b) is the as-recorded high resolution image showing the interface between a ZnO grain and a Pt grain. The ZnO (0002) planes are grown on top of the Pt (111) plane with a very clean interface. There is a noticeable diffusion between the Pt layer and the Si substrate shown in the low magnification image. The energy-dispersive x-ray spectroscopy studies (data not shown) confirmed that the interfacial region between Pt and Si contains an alloy of Pt and Si with various degrees of mixing. There is no evidence, however, that the diffusion had influenced the growth of ZnO and other Pt layers.

Due to the good crystallinity and textured structure, our ZnO film was found to exhibit a large stiffness and good electromechanical coupling property in the piezoelectric measurements (data not shown). The resonant frequencies of the bare FBAR devices were determined and the results are shown in Fig. 3 (the pattern of top electrodes is shown in the inset). As a comparison, the resonant frequency of the devices with different ZnO thicknesses was calculated based on Eq. (1) and using literature data for $k_t^2=8.5\%$, c_{33}^E

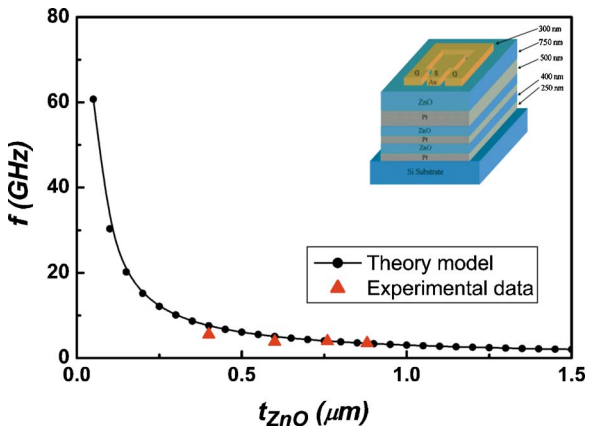

FIG. 3. (Color online) Resonance frequency of ZnO-FBAR. The inset shows the schematic structure of the device.

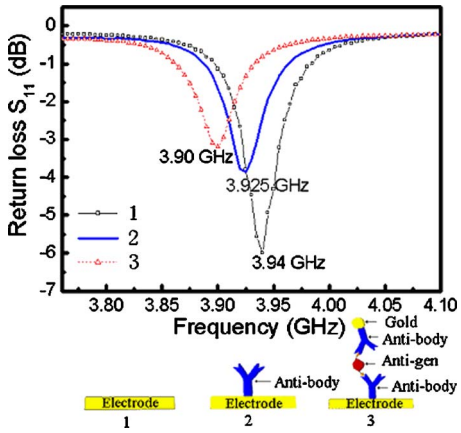

FIG. 4. (Color online) Return loss (S_{11}) of ZnO FBAR (1) bare device, (2) after bioimmobilization and (3) after protein coupling.

$=210$ GPa, and $\rho=5.7\times10^3$ kg/m^3.[12–14] A good agreement between the experimental data and calculation results was found. For our FBAR device with ZnO thickness=750 nm, for example, the measured resonant frequency was 3.94 GHz while the theoretical value was 4.08 GHz. The difference between these two results is only ~3.5%. Samples with different ZnO thicknesses were also prepared and tested, as shown in Fig. 3.

The use of the FBAR in the detection of coating mass is demonstrated in Fig. 4. The return loss (S_{11}) of devices with/without coatings was characterized on a network analyzer. As shown in Fig. 4, three featured frequencies were observed: (1) the resonant frequency of the bare device, $f_r=3.940$ GHz; (2) after bioimmobilization (i.e., with the coating of antibody), $f_r'=3.925$ GHz; and (3) after the protein coupling (i.e., with the addition of more bioappending mass), $f_r''=3.900$ GHz. The difference in resonant frequency between FBAR for different bioattaching cases is ~20 MHz, which is large enough for conventional detection. The bioappending mass can be estimated by using the Sauerbrey equation[20]

$$\Delta m = -(A\sqrt{\rho\mu}/2f_r^2)\Delta f, \tag{2}$$

where Δm, A, ρ, μ, f_r, and Δf are the appending mass, area, density, elastic constant, fundamental resonant frequency and frequency shift, respectively. By calculation, we have found that the bioimmobilization mass and the mass of protein through coupling were 380 and 630 pg, respectively. These results are in good agreement with the results that were estimated based on the known concentrations and volumes of the solutions used for the coatings. According to definition of sensitivity,[3,6] $S=(\partial f/\partial m)$, the calculated sensitivity of our biosensor is 8970 Hz cm^2/ng, which is obviously much larger than the conventional QCMs.

In summary, a ZnO-based film bulk acoustic resonator has been fabricated through an optimized magnetron sputtering process. By x-ray diffraction, atomic force microscope, and transmission electron microscope observations, it was found that all thin film layers (ZnO and Pt) were well crystallized, highly oriented, smooth, and uniform. The electrical measurements revealed that the FBAR consisting of a 750 nm thick ZnO layer was featured with a high resonant frequency of 3.94 GHz. A large shift of the resonant frequency was observed as different biospecies were coated on the device. The sensitivity of the FBAR device, estimated based on the experiments, was ~8970 Hz cm^2/ng.

This work was supported by the Chinese Academy of Sciences (Y2005027), Shanghai Commission of Science and Technology (0452nm012, 04ZR14154, 04JC14080, 05JC14076, AM0414, 0552nm043, AM0517, and 06QA14060), and the Hong Kong Polytechnic University (ICRG A-PG18 and G-YF01). Support from the Center for Smart Materials of the Hong Kong Polytechnic University is also acknowledged.

[1] K. M. Lakin, IEEE Microw. Mag. **4**, 61 (2003).
[2] R. Lanz and P. Muralt, IEEE Trans. Ultrason. Ferroelectr. Freq. Control **52**, 936 (2005).
[3] C. Kößlinger, S. Drost, F. Aberl, H. Wolf, S. Koch, and P. Woias, Biosens. Bioelectron. **7**, 397 (1992).
[4] H. P. Löbl, M. Klee, R. Milsom, R. Dekker, C. Metzmacher, W. Brand, and P. Lok, J. Eur. Ceram. Soc. **21**, 2633 (2001).
[5] S. H. Lee, K. H. Yoon, and J. K. Lee, J. Appl. Phys. **92**, 4062 (2002).
[6] R. Gabl, H. D. Feucht, H. Zeininger, G. Eckstein, M. Schreiter, R. Primig, D. Pitzer, and W. Wersing, Biosens. Bioelectron. **19**, 615 (2004).
[7] C. S. Lu, *Applications of Piezoelectric Quartz Crystal Microbalance* (Elsevier, London, 1984), Vol. 7, pp. 1–5.
[8] L. Mai, D. H. Kim, M. Yim, and G. Yoon, Microwave Opt. Technol. Lett. **42**, 505 (2004).
[9] T. Zhang, Y. Wang, W. L. Liu, J. G. Cheng, Z. T. Song, S. L. Feng, H. L. W. Chan, and C. L. Choy, Chin. Phys. Lett. **22**, 694 (2005).
[10] L. Yan, W. Pang, E. S. Kim, and W. C. Tang, Appl. Phys. Lett. **87**, 154103 (2005).
[11] H. Zhang and E. S. Kim, J. Microelectromech. Syst. **14**, 699 (2005).
[12] K. L. Ekinci, Y. T. Yang, and M. L. Roukes, J. Appl. Phys. **95**, 2682 (2004).
[13] H. Campanella, J. Esteve, J. Montserrat, A. Uranga, G. Abadal, N. Barniol, and A. Romano-Rodríguezs, Appl. Phys. Lett. **89**, 033507 (2006).
[14] M. Hara, J. Kuypers, T. Abe, and M. Esashi, Sens. Actuators, A **117**, 211 (2005).
[15] S. R. Mermet, R. Lanz, and P. Muralt, Sens. Actuators B **114**, 681 (2006).
[16] M. Schreiter, R. Gabl, D. Pitzer, R. Primig, and W. Wersing, J. Eur. Ceram. Soc. **24**, 1589 (2004).
[17] K. M. Lakin, IEEE Microw. Mag. **4**, 61 (2003).
[18] U. Ozgur, Y. I. Alivov, C. Liu, A. Teke, M. A. Reshchikov, S. Dogan, V. Avrutin, S. J. Cho, and H. Morkoc, J. Appl. Phys. **98**, 041301 (2005).
[19] G. Carlotti, G. Socino, A. Petri, and E. Verona, Appl. Phys. Lett. **51**, 1889 (1987).
[20] A. Rahtu and M. Ritala, Appl. Phys. Lett. **80**, 521 (2002).